



Copper(II) thenoyltrifluoroacetate as acceptor matrix in design of heterospin complexes

Ilia Yeltsov ^b, Victor Ovcharenko ^{a,*}, Vladimir Ikorskii ^a, Galina Romanenko ^a,
Sergei Vasilevsky ^a

^a International Tomography Center, Russian Academy of Sciences, Institutskaya Str. 3A, 630090 Novosibirsk, Russia

^b Novosibirsk State University, Pirogova Str. 2, 630090 Novosibirsk, Russia

Received 17 September 2000; accepted 15 October 2000

Abstract

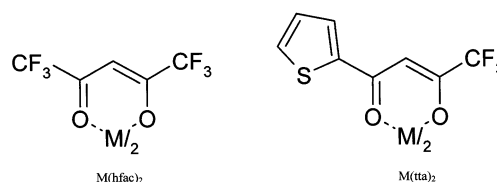
Coordination compounds of Cu(II) thenoyltrifluoroacetate with stable 2-imidazoline nitroxides were synthesized; their structure and magnetic properties were investigated. The complex with a pyrazole nitroxide was isolated as two polymorphous modifications. For both polymorphs, the structure is comprised of $\text{Cu}(\text{tta})_2(\text{NITPz}^{1,3\text{Me}})$ molecules shaped as nearly regular pyramids with four O atoms of the two tta ligands lying at the base. The solid polymorphs are constructed from formal binuclear fragments appearing when the pyramid bases of two neighboring molecules approach each other forming rather short contacts Cu–S (3.848 and 3.596 Å), due to which the polymorphs differ considerably in magnetic properties. In the modification with longer Cu–S distances, there are no exchange interactions between the paramagnetic centers of the neighboring $\text{Cu}(\text{tta})_2(\text{NITPz}^{1,3\text{Me}})$ molecules whereas in the polymorph with shorter Cu–S distances the interactions are significant and analogous to those in real dimer molecules based on the $\text{Cu}(\text{AcO})_2$ matrix with a nitroxide. © 2001 Elsevier Science Ltd. All rights reserved.

Keywords: Copper(II); Nitroxide; Dimers; Polymorphous modifications

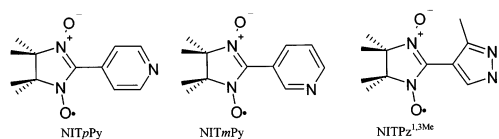
1. Introduction

Metal hexafluoroacetylacetonates are widely used as acceptor matrices for syntheses of heterospin systems [1] (Scheme 1). Due to their stereochemical nonrigidity, the matrices form heterospin complexes with polyfunctional nitroxides varying in composition and structure and showing the ability for magnetic ordering [2–6]. For the $\text{Cu}(\text{hfac})_2$ complex with nitronyl nitroxide containing a pyridine substituent in the 2-position of the imidazoline heterocycle (NITmPy), a new type of thermally induced spin transition was found [7]. We attempted to expand the scope of Cu-containing matrices which are capable of forming heterospin complexes with nitroxides (Schemes 1 and 2). Copper(II) thenoyltrifluoroacetate, $\text{Cu}(\text{tta})_2$, related to $\text{Cu}(\text{hfac})_2$, was

chosen as an acceptor matrix and the widely used NITpPy and NITmPy as well as the pyrazole derivative $\text{NITPz}^{1,3\text{Me}}$, structurally related to NITmPy, were chosen as nitronyl nitroxides. Since $\text{Cu}(\text{tta})_2$ and $\text{Cu}(\text{hfac})_2$ exhibit similarity in their accepting abilities and in the



Scheme 1.



Scheme 2.

* Corresponding author. Fax: +7-3832-331399.

E-mail address: ovchar@tomo.nsc.ru (V. Ovcharenko).

structure of coordination site, $\text{Cu}(\text{tta})_2$ was expected to behave analogously to $\text{Cu}(\text{hfac})_2$ with nitroxides. It appeared, however, that $\text{Cu}(\text{tta})_2$, which is stereochemically more rigid, reacts with pyridine-containing nitronyl nitroxides typically forming much fewer types of heterospin complex compared to $\text{Cu}(\text{hfac})_2$. In reaction with a pyrazole-substituted nitronyl nitroxide, $\text{Cu}(\text{tta})_2$ gave a heterospin compound with an unknown structure whose magnetic behavior resembles that of the binuclear complex $[\text{Cu}(\text{AcO})_2]_2(\text{NITpPy})_2$. Here we report on syntheses, structure, and magnetic properties of all of the isolated $\text{Cu}(\text{tta})_2$ complexes with the above nitronyl nitroxides.

2. Experimental

2.1. Nitronyl nitroxides

The nitronyl nitroxides used in this work were synthesized by known procedures [8,9]. 2,3-Dihydroxy-lamino-2,3-dimethylbutane sulfate needed for syntheses of nitroxides was prepared according to [10,11].

2.2. Syntheses of complexes

2.2.1. $\text{Cu}(\text{tta})_2(\text{NITpPy}) \cdot 0.5\text{C}_6\text{H}_6$ (I)

$\text{Cu}(\text{tta})_2$ (216 mg, 0.43 mmol) was dissolved in ethylacetate (5 ml). To the resulting solution was added a solution of NITpPy (100 mg, 0.43 mmol) in benzene (10 ml) and the mixture was allowed to stay in an open container at room temperature (r.t.). The solution evaporated to half of its volume within three days, whereupon a green precipitate settled out which was filtered off and washed with a cool hexane–benzene mixture. The product was recrystallized from benzene from which it was separated as single crystals suitable for an X-ray diffraction analysis. Yield 255 mg (77%). $T_m = 166\text{--}167^\circ\text{C}$. IR spectrum (cm^{-1}): 3436; 3106; 1593; 1532; 1410; 1316; 1144; 787; 730. *Anal.* Found: C, 46.6; H, 3.3; N, 5.4; F, 15.3. Calc. for $\text{CuC}_{31}\text{H}_{35}\text{N}_3\text{O}_6\text{F}_6\text{S}_2$: C, 45.5; H, 3.3; N, 5.7; F, 15.4%. Using other starting ratios of $\text{Cu}(\text{tta})_2/(\text{NITpPy})$ in the reaction mixture also led to crystallization of I.

2.2.2. $\text{Cu}(\text{tta})_2(\text{NITmPy})_2 \cdot \text{C}_7\text{H}_8$ (II)

Toluene (10 ml) was poured into a mixture of $\text{Cu}(\text{tta})_2$ (216 mg, 0.43 mmol) and NITmPy (100 mg, 0.43 mmol). The mixture was stirred at r.t. for 2 h. The resulting solution was filtered, heptane (5 ml) was added to the filtrate, and the solution was allowed to stay at r.t. After 4 days, concretions of greenish blue crystals formed on the walls of the container, which were separated and washed with heptane. Slow evaporation of the mother solution gave more product as single crystals suitable for an X-ray diffraction analysis.

Yield 200 mg (60%). $T_m = 90\text{--}92^\circ\text{C}$. IR spectrum (cm^{-1}): 3097; 2994; 2943; 1621; 1536; 1413; 1399; 1371; 1287; 1240; 1142; 779; 696. *Anal.* Found: C, 52.4; H, 4.7; N, 7.9; F, 11.0; S, 5.9. Calc. for $\text{CuC}_{47}\text{H}_{48}\text{N}_6\text{O}_8\text{F}_6\text{S}_2$: C, 52.9; H, 4.5; N, 7.9; F, 10.7; S, 6.0%.

2.2.3. $\text{Cu}(\text{tta})_2(\text{NITPz}^{1,3\text{Me}})$ (III and IV)

A mixture of $\text{Cu}(\text{tta})_2$ (100 mg, 0.2 mmol) and 50 mg (0.2 mmol) $\text{NITPz}^{1,3\text{Me}}$ was dissolved in a (10/3) hexane–ethylacetate mixture with stirring and heating to 50°C for 1 h. The solution was then cooled to r.t. and allowed to stay for 2 days. Dichroic (blue–green) single crystals (denoted by IV) shaped as long needles formed in the solution. The mother solution was decanted and allowed to stay, and crystals IV (25 mg) were collected and dried on a paper filter. Rhomboid dark blue crystals (III) (90 mg) precipitated from the mother solution which was stored for 3 days more at r.t. Note that III was the major product in all syntheses. In some cases, IV was not detected at all, and the whole solid consisted of crystals III. Solids III and IV have the same composition since they are polymorphous modifications of $\text{Cu}(\text{tta})_2(\text{NITPz}^{1,3\text{Me}})$. Therefore, the results of analysis are given for only one modification (III). *Anal.* Found: C, 45.4; H, 3.8; N, 7.51; F, 15.8; S, 8.3. Calc. for $\text{CuC}_{28}\text{H}_{27}\text{N}_4\text{O}_6\text{F}_6\text{S}_2$: C, 44.4; H, 3.6; N, 7.40; F, 15.1; S, 8.5%. For III: $T_m = 167\text{--}168^\circ\text{C}$; IR spectrum (cm^{-1}): 3086; 2991; 1593; 1543; 1411; 1360; 1316; 1233; 1190; 1147; 941; 786; 594; 540; 466. For IV: $T_m = (139\text{--}144^\circ\text{C}$, color change) $159\text{--}160^\circ\text{C}$, melting with decomposition; IR spectrum (cm^{-1}): 3439; 3062; 2996; 1613; 1586; 1542; 1413; 1354; 1316; 1232; 1198; 1178; 1149; 1067; 940; 787; 592; 540; 465.

2.2.4. $[\text{Cu}(\text{AcO})_2]_2(\text{NITpPy})_2$ (V)

$\text{Cu}(\text{AcO})_2 \cdot \text{H}_2\text{O}$ (85 mg, 0.43 mmol) was dissolved with prolonged stirring at r.t. in methanol (15 ml). Then NITpPy (100 mg, 0.44 mmol) was added to the reaction mixture while stirring was continued. A finely dispersed green precipitate started to settle from the reaction mixture within a few moments. Stirring was continued for further 3 h. The precipitate was filtered off, washed with toluene to remove the excess of radical (until the solvent ceased to show color), and dried in air. Yield 120 mg (67%). $T_m = 218\text{--}219^\circ\text{C}$. IR spectrum (cm^{-1}): 2991; 2942; 1623; 1427; 1312; 1215; 1167; 1066; 1016; 834; 681; 626; 542; 460. *Anal.* Found: C, 46.5; H, 5.3; N, 10.0. Calc. for $\text{CuC}_{16}\text{H}_{22}\text{N}_3\text{O}_6$: C, 46.2; H, 5.3; N, 10.1%. To grow perfect single crystals of $\text{Cu}_2(\text{AcO})_4(\text{NITpPy})_2$, $\text{Cu}(\text{AcO})_2 \cdot \text{H}_2\text{O}$ was dissolved in boiling methanol, the solution was then cooled to 30°C , and an equal amount of NITpPy was added. Toluene was added to the resulting dark blue solution until the methanol/toluene ratio became 2/1, and the solution was allowed to stay in an open flask at r.t. for 5 days.

Table 1

	I	II	III	IV	V
Structural motif	Chain 'head-to-head'	Molecular	'Dimer-like'	'Dimer-like'	Dimer
Cu–O _{NIT}	2.458(2)				
Cu–N _{NIT}	2.035(2)	2.033(2)	2.428(3)	2.366(12)	2.144(5)
Cu–O _{tta}	1.924(1), 1.931(2), 2.020(2), 2.170(2)	1.973(2), 2.262(2)	1.921(3), 1.933(3), 1.925(3), 1.939(3)	1.924(8), 1.934(9), 1.943(8), 1.932(8)	1.956(5), 1.974(5), 1.966(4), 1.954(4)
N–O	1.261(2), 1.278(2)	1.282(3), 1.277(3)	1.281(6), 1.275(6)	1.268(15), 1.255(15)	1.293(6), 1.267(6)
∠ Py(Pz)–CN ₂	16.7	22.0	37.3	39.7	24.2

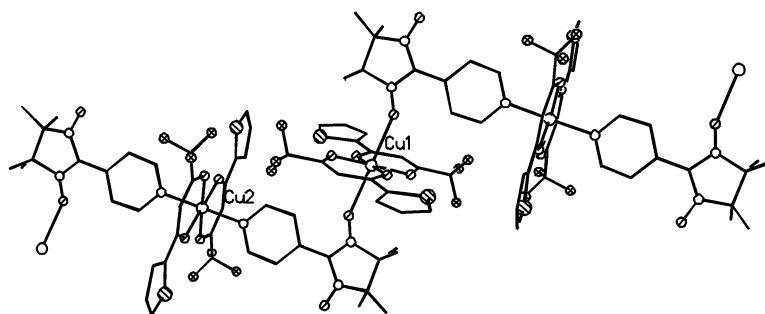


Fig. 1. Structure of the chain in I (benzene molecules and hydrogen atoms omitted for clarity).

The solution evaporated to half of its volume, and perfectly shaped bright green plates of the complex gradually grew in it. The plates were filtered off, washed with toluene, and dried in air.

2.3. Magnetic measurements

Magnetic susceptibilities of the complexes were measured on an MPMS-5S (Quantum design) SQUID magnetometer at temperatures of 2–300 K and in magnetic fields of up to 10 kOe. The calculated temperature-dependent paramagnetic susceptibility was corrected for the diamagnetic term, which was $372 \times 10^{-6} \text{ cm}^3 \text{ mol}^{-1}$ for **III**, **IV** and $191 \times 10^{-6} \text{ cm}^3 \text{ mol}^{-1}$ for $[\text{Cu}(\text{AcO})_2]_2(\text{NIT}p\text{Py})_2$, and for the temperature-independent paramagnetic contribution of the Cu(II) ion, which was $60 \times 10^{-6} \text{ cm}^3 \text{ mol}^{-1}$. The effective magnetic moment was calculated by the formula $\mu_{\text{eff}} = (3k/N\beta^2 \cdot \chi T)^{1/2}$.

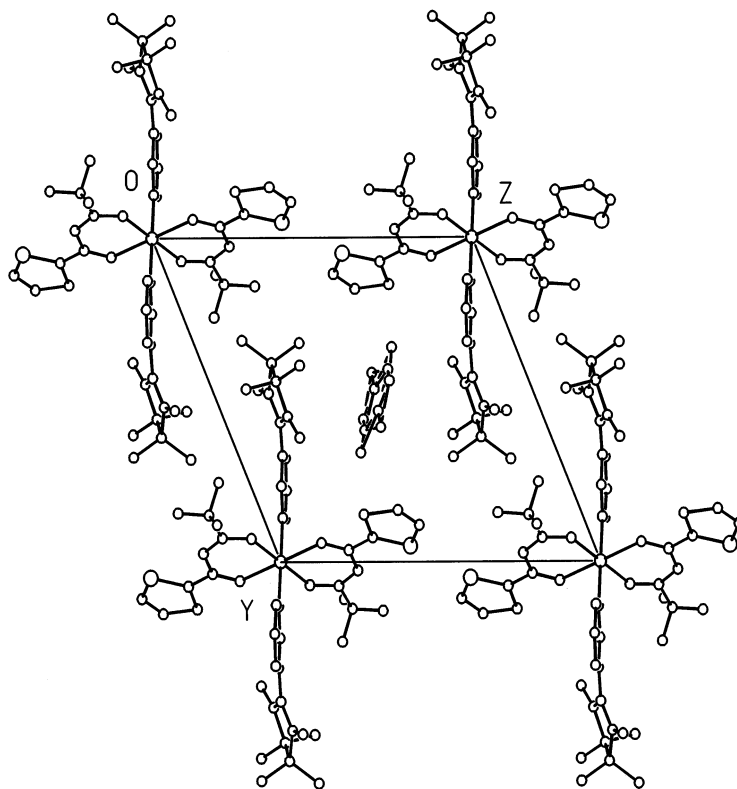
2.4. X-ray crystallography

Crystals **I–V** are triclinic. The data were collected on ENRAF NONIUS CAD4 and BRUKER AXS P4 automatic diffractometers using standard methods (Mo K α radiation, graphite monochromator, $\theta/2\theta$ scan mode, variable scan speed). The structures were solved with SIR-97 and refined anisotropically for all nonhydro-

gen atoms. H atoms were partly located on difference electron density maps (the others were calculated geometrically) and refined isotropically. The crystal data needed for further discussion are given in Table 1.

3. Results and discussion

Our study of the reaction products of $\text{Cu}(\text{tta})_2$ with $\text{NIT}p\text{Py}$ and $\text{NIT}m\text{Py}$ led to compounds of composition $\text{Cu}(\text{tta})_2(\text{NIT}p\text{Py}) \cdot 0.5\text{C}_6\text{H}_6$ and $\text{Cu}(\text{tta})_2(\text{NIT}m\text{Py})_2 \cdot \text{C}_7\text{H}_8$. No complexes with other stoichiometries have been detected. Although $\text{NIT}p\text{Py}$ and $\text{NIT}m\text{Py}$ are functionally related, in reaction with $\text{Cu}(\text{tta})_2$ they form complexes which have essentially different structures in the solid state. The two crystallographically independent Cu atoms in the structure of **I** have a centrosymmetric distorted octahedral environment (Fig. 1). The O_{tta} atoms lie in the equatorial plane of a pulled tetragonally distorted Cu1 octahedron ($\text{Cu}–\text{O}_{\text{tta}}$ distances are 1.924(1) and 1.931(2) Å); the nitroxyl O atoms of $\text{NIT}p\text{Py}$ are in the axial positions forming $\text{Cu}–\text{O}_{\text{NIT}}$ distances of 2.458(2) Å and a $\text{Cu}–\text{O}–\text{N}$ angle of $146.1(1)^\circ$. For the Cu2 atom, the equatorial plane of a nearly isometric octahedron is formed by two N atoms of the pyridine heterocycle ($\text{Cu}–\text{N}_{\text{NIT}}$ 2.035(2) Å) and two O_{tta} atoms ($\text{Cu}–\text{O}$ 2.020(2) Å), the other two O_{tta} atoms occupying the axial positions ($\text{Cu}–\text{O}$

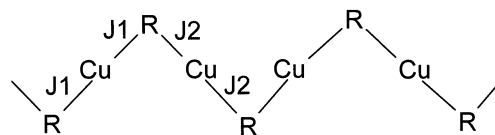
Fig. 2. Structure of **II**.

2.170(2) Å) (Table 1). The N–O distance in the coordinated fragment is slightly shorter (1.261(2) Å) than that in the noncoordinated N–O group (1.278(2) Å). The tta fragments, which are trans to each other, are nearly planar, the angle between the thenoyl heterocycle and the respective metallocycle being up to 7.6°. The angle between the planes of the Py ring and the CN₂ fragment of the imidazoline heterocycle is 16.7°. The paramagnetic NITpPy performs the bridging function, linking the Cu(tta)₂ fragments into infinite zigzag chains having a ‘head-to-head’ motif and running along [1̄01]. The space between the chains is occupied by the benzene molecules.

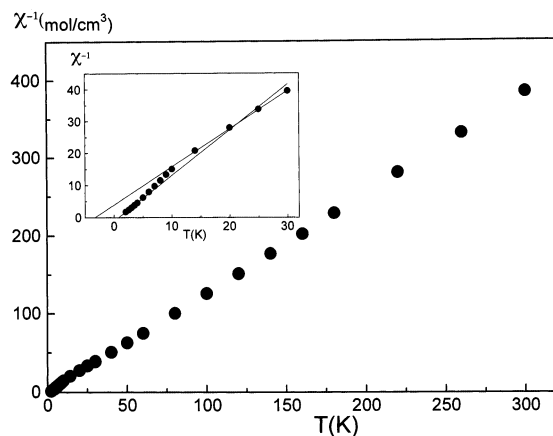
The structure of solid **II** is much simpler. It is built from discrete Cu(tta)₂(NITmPy)₂ fragments alternating with the toluene molecules (Fig. 2). The centrosymmetric distorted octahedral environment of the copper atom is formed in the equatorial plane by the N atoms of the pyridine heterocycles (Cu–N_{NIT} 2.033(2) Å) and by two O_{tta} atoms (Cu–O 1.973(2) Å). The axial positions are occupied by the other two O_{tta} atoms (Cu–O 2.262(2) Å).

Analyzing the magnetic properties of **I**, we correlated the polymer chain to the following scheme of exchange channels $J_1(\text{Cu}-\text{O}\cdots\text{N}<)$ and $J_2(\text{Cu}\cdots>\text{N}-\text{O})$ (Scheme 3).

On the $\chi^{-1}(T)$ curve (Fig. 3), one can isolate two linear segments corresponding to different parameters of the Curie–Weiss equation $\chi(T) = C/(T - \theta)$:



Scheme 3.

Fig. 3. Dependence $\chi^{-1}(T)$ for **I**.

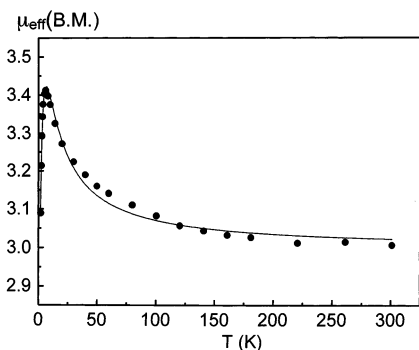


Fig. 4. Theoretical (solid line) and experimental temperature dependences of μ_{eff} for **II**.

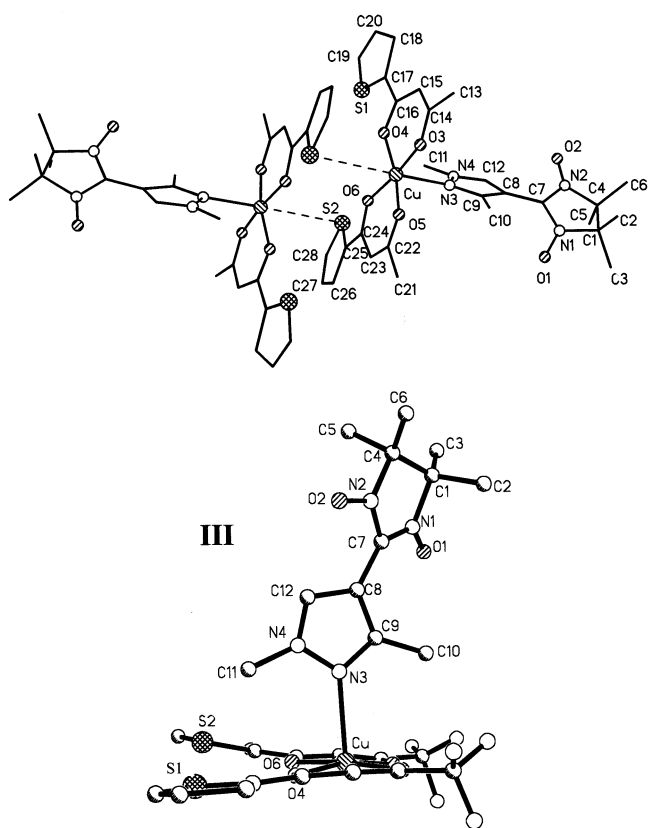


Fig. 5. View of molecule **III**.

$T < 4$ K, $C = 0.703$, $\theta = 0.77$ K

$T > 10$ K, $C = 0.785$, $\theta = -3.3$ K

The exchange parameters were qualitatively estimated by the formula $\theta = 2zJS(S+1)/3k$ [12] in a molecular field approximation: $J_1 = 0.54$ cm^{-1} and $J_2 = -2.3$ cm^{-1} . The J_1 parameter may be assigned to the head-to-head fragment $>N\cdot O-Cu-O\cdot-N<$ since ferromagnetic exchange is characteristic for Cu^{2+} complexes with an axial coordination of the nitroxyl group. The low value of ferromagnetic exchange may be the consequence of the long distance between the copper atom

and the coordinated nitroxyl oxygen (Table 1). The exchange interactions by the J_2 channel, i.e. through the pyridine heterocycle are much more pronounced.

The possibility of strong exchange interactions of odd electrons through the pyridine heterocycle is supported by the results of studies on molecular complex **II** in which the shortest intermolecular contacts between the O atoms of the $O-N<$ fragments are up to 4.4 Å. Therefore, the crystal structure of **II** may be regarded as comprised of quasiisolated exchange clusters $O-N<\cdots Cu^{2+}\cdots >N\cdot O$ with indirect interactions via the N atom of the pyridine ring. Theoretical treatment of the experimental dependence $\mu_{\text{eff}}(T)$ for **II** (Fig. 4) was carried out on a three-center heterospin exchange cluster model [13]. The energy levels of the cluster in an external magnetic field were calculated using the isotropic spin Hamiltonian:

$$\hat{H} = -2J\hat{s}\hat{s}' - \beta(g_{\text{Cu}}\hat{S}_z + g_L\hat{S}_z)H - 2J'z\hat{S}_z\langle\hat{S}_z\rangle$$

where J and $J'z$ are the intra and intercluster exchange parameters, \hat{s} is the Cu^{2+} spin operator, $\hat{s} = \hat{s}_1 + \hat{s}_2$ is the operator of the total spin of two radicals, g and g' are the g factors of Cu^{2+} and nitroxide, z is the number of the nearest-neighbor molecules, β the Bohr magneton, $\hat{S} = \hat{s} + \hat{s}'$ is the operator of the total spin of the cluster, and $\langle\hat{S}_z\rangle$ is its averaged projection onto the z axis. The optimal J , $J'z$, and g_{Cu} ($g_L \equiv 2$) values were obtained by minimization of $\sum_i [\mu_{\text{eff}}^{\text{calc}}(T_i) - \mu_{\text{eff}}^{\text{measd}}(T_i)]^2$. The optimization gave the following spin Hamiltonian parameters: $g = 2.00 \pm 0.01$, $J = 6.1 \pm 0.01$ cm^{-1} , $J'z = -0.31 \pm 0.05$ cm^{-1} , indicative of appreciable ferromagnetic exchange interactions in the cluster. The opposite sign of the exchange parameter (J for **II** and J_2 for **I**) is in good agreement with spin polarization effects.

Although $\text{NITPz}^{1,3\text{-Me}}$ is related to NITmPy in the sequence of donor atoms in the paramagnetic ligand, in reactions with $\text{Cu}(\text{tta})_2$ at different reagent ratios it forms only a 1:1 complex $\text{Cu}(\text{tta})_2(\text{NITPz}^{1,3\text{Me}})$. This compound was isolated as two polymorphous modifications (**III** and **IV**). In both structures, the environment of the Cu atom is a square pyramid with four O atoms of two tta ligands at the base ($\text{Cu}-\text{O}_{\text{tta}}$ 1.921(3)–1.943(8) Å) and the pyrazole N atom at the apex (Figs. 5 and 6). Also note that the tta ligands are *cis* to each other. The Cu–N distances differ widely: 2.428(3) in **III** and 2.366(12) Å in **IV**. The greatest differences between the molecular geometries of **III** and **IV** are observed in the values of torsion angles (Table 2).

The $\text{Cu}(\text{tta})_2\text{NITPz}^{1,3\text{Me}}$ molecules are linked into dimer-like fragments by weak $\text{Cu}\cdots\text{S}$ contacts, increasing the coordination number of copper to 6. The differences in molecular geometry cause significant differences in intermolecular contacts: $\text{Cu}\cdots\text{S}$ 3.848 and 3.596 Å, $\text{N1-O1}\cdots\text{O1}'-\text{N1}'$ 4.372 and 3.454 Å, $\text{N2-O2}\cdots\text{O1}'-\text{N1}'$ 4.962 and 4.631 Å, $\text{Cu}\cdots\text{Cu}$ 5.547 and

6.805 Å for **III** and **IV**, respectively, and in the magnetic behavior of these modifications.

The absence of a temperature dependence for μ_{eff} in the range 2–300 K for **III** (Fig. 7) points to very weak indirect exchange interactions between the odd electrons of the copper ion and the nitroxyl group occurring via the pyrazole heterocycle of a separate fragment of $\text{Cu}(\text{tta})_2(\text{NITPz}^{1,3\text{Me}})$ in agreement with considerably longer $\text{Cu}-\text{N}_{\text{NIT}}$ distance compared to that in the above complexes with pyridine-substituted nitroxides (Table 1). The intermolecular exchange interactions in solid **III** are not observed below 2 K. Magnetic susceptibility of **III** is well approximated by the Curie equation

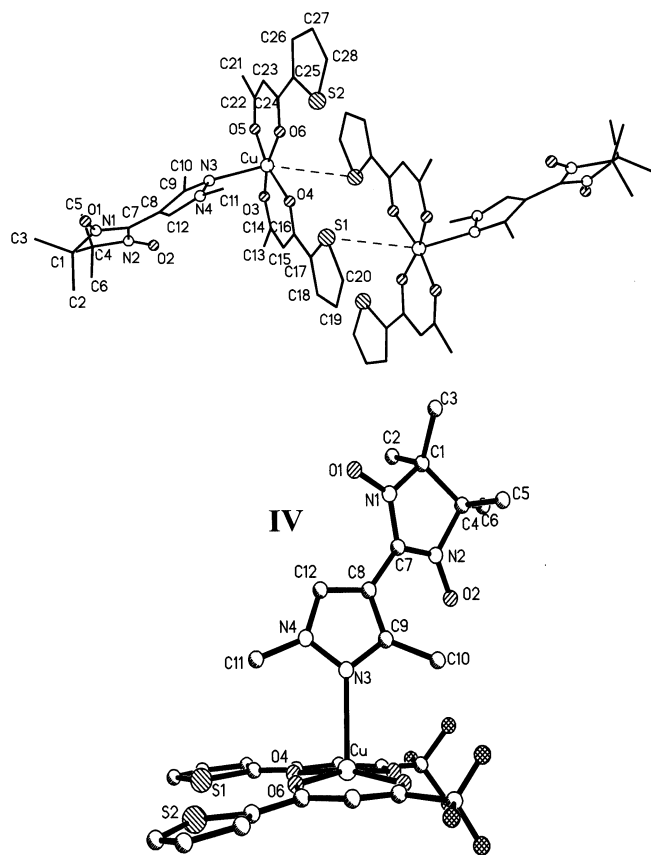


Fig. 6. View of molecule **IV**.

Table 2
Selected torsion angles

Atoms	Torsion angles (°)	
	III	IV
S1C17C16O4	−4.1	9.1
S2C25C24O6	7.2	−3.2
O4CuN3N4	29.6	57.9
O6CuN3N4	−58.9	−28.6
C12C7C7N2	−141.8	34.8
C12C7C7N1	39.0	−138.7

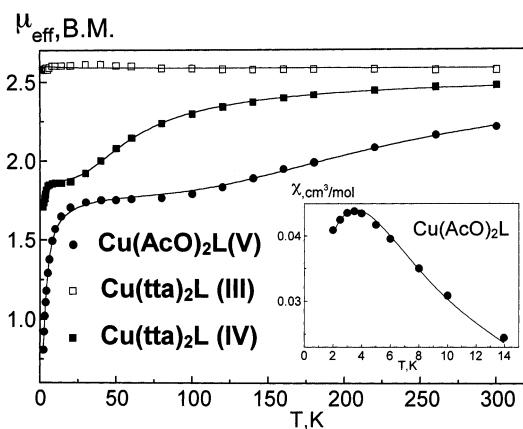


Fig. 7. Dependences $\mu_{\text{eff}}(T)$ for **III–V**. Solid lines: theoretical dependences described in the text. Insert: Dependence $\chi(T)$ for **V**.

tion $\chi = N\beta^2\mu_{\text{eff}}^2/3kT = C/T$ with a constant $C = 0.83$.

In **IV** having much shorter $\text{Cu}-\text{S}$ and $\text{Cu}-\text{Cu}$ distances in the dimer-like fragment $\{(\text{NITPz}^{1,3\text{Me}})-(\text{tta})_2\text{Cu}\cdots\text{Cu}(\text{tta})_2(\text{NITPz}^{1,3\text{Me}})\}$ compared to **III**, the exchange interactions between the paramagnetic centers are much more effective. The experimental curve $\mu_{\text{eff}}(T)$ for **IV** is formally divided into three sections. At low temperatures, the effective magnetic moment slightly increases with temperature. The region where the dependence $\mu_{\text{eff}}(T)$ is absent and $\mu_{\text{eff}} \sim 1.8$ BM is followed by the section where μ_{eff} increases with temperature up to RT . An analysis of structural data and $\mu_{\text{eff}}(T)$ makes it possible to represent the experimental $\mu_{\text{eff}}(T)$ curve as the sum of two major exchange interaction terms, differing widely in magnitude. In the high-temperature region, the curve is well approximated by the model of the $\text{Cu}(\text{II})-\text{Cu}(\text{II})$ dimer whose magnetic susceptibility is defined by the Bleaney–Bowers equation:

$$\chi_{\text{dim}} = \frac{N\beta^2 g_{\text{Cu}}^2}{3kT} \left[1 + \frac{1}{3} \exp\left(\frac{-2J}{kT}\right) \right]^{-1}$$

and at low temperatures depends on the weak exchange interactions between the radicals J_1 ($J_1 \ll J$). Magnetic susceptibility in this region obeys the Curie–Weiss law with a low Weiss constant $\chi = C/(T - \theta)$. The results of the approximation of the experimental dependence by the sum:

$$\chi = \chi_{\text{dim}} + C/(T - \theta)$$

with the optimal parameters $g_{\text{Cu}} = 2.0$, $J = -45 \text{ cm}^{-1}$, $C = 0.906$, and $\theta = -0.5$ are presented in Fig. 7. The value of $\mu_{\text{eff}} \sim 1.8$ BM in the ‘intermediate’ region indicates that at $T < 20$ K complete spin coupling takes place in the exchange-coupled dimer $\text{Cu}-\text{Cu}$ and that the major contribution to μ_{eff} is from the paramagnetic centers of nitroxides.

In order to justify the use of the Cu–Cu dimer model in treatment of the magnetic properties of **IV**, we synthesized the authentic dimer **V** and investigated its magnetic properties. This molecule (Fig. 8) is really a dimer which is centrosymmetric relative to the middle of the Cu–Cu bond.

The square bipyramid around the Cu atom consists of four oxygen atoms of the acetate ligands in the equatorial plane and the second Cu atom of the dimer and the pyridine N atom in the axial positions. The Cu–O, Cu–Cu, and Cu–N distances are 1.54(4)–1.974(5), 2.617(2), and 2.144(5) Å, respectively. The bond lengths and angles in the bridging acetate ligands agree with the values cited in the literature: C–O 1.244(7)–1.253(7), C–C 1.503(11)–1.532(1) Å; \angle OCO 126.4(7) and 127.3(6)°. In the structure of nitronyl nitroxide fragments, the N–O bond lengths differ considerably (Table 1). The plane of the Py ring makes an angle of 82.1° with the equatorial plane of the Cu bipyramid and an angle of 24.2° with the N(1)C(3)N(2) plane of the imidazoline heterocycle. The structure of **V** in general is considered molecular. It has rather short contacts between the O atoms of the N–O groups of the neighboring dimer molecules (3.727 and 4.042 Å). This was taken into consideration in treatment of the experimental dependence $\mu_{\text{eff}}(T)$ for **V** (Fig. 7).

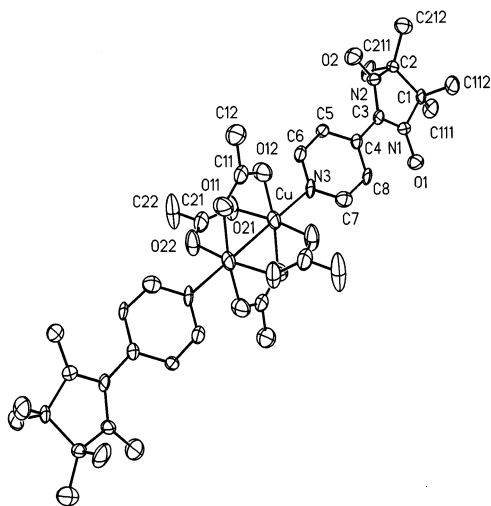
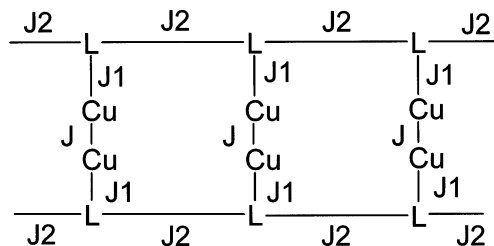


Fig. 8. Structure of dimer molecule **V**.



Scheme 4.

The form of the $\mu_{\text{eff}}(T)$ curve for **V** suggests that there are stronger antiferromagnetic exchange interactions in the Cu–Cu dimer compared to **IV**. The magnetic susceptibility $\chi(T)$ curve for **V**, however, is distinctive at low temperatures, having a broad maximum (Fig. 7, insert) indicative of antiferromagnetic ordering typical for a polymer chain. Using the crystal data for **V**, one can represent the exchange interactions between the paramagnetic centers in this complex as shown in Scheme 4.

The above magnetic data for **I**, **III**, and **IV** are used to make estimates $J \gg J_2 > J_1$, which are readily evident. In the framework of this exchange coupling scheme, the dependence $\mu_{\text{eff}}(T)$ for **V** is exclusively dominated by the J_2 interactions between the radicals of different molecules in the chains at low temperatures and by the exchange interactions between the Cu(II) ions via the carboxylate bridges in the dimers at high temperatures. Therefore, magnetic susceptibility of **V** is represented as the sum of the magnetic susceptibilities of the exchange-coupled Cu–Cu dimer and the exchange chain [14,15]:

$$\chi = \chi_{\text{chain}} + \chi_{\text{dim}}$$

where

$$\chi_{\text{dim}} = \frac{N\beta^2 g_{\text{Cu}}^2}{3kT} \left[1 + \frac{1}{3} \exp\left(\frac{-2J}{kT}\right) \right]^{-1}$$

$$\chi_{\text{chain}} = \frac{N\beta^2 g_{\text{R}}^2}{kT} \cdot \frac{0.25 + Bx + Cx^2}{1 + Dx + Ex^2 + Fx^3}$$

where $x = |J_2|/kT$. This coupling scheme nicely approximates the experimental dependence (Fig. 7); the optimal theoretical curve is characterized by the following parameters: $g_{\text{R}} = 2.07$, $J_2 = -2 \text{ cm}^{-1}$; $g_{\text{Cu}} = 2.18$, $J = -181 \text{ cm}^{-1}$.

4. Supplementary material

Crystallographic data for the structural analysis have been deposited with the Cambridge Crystallographic Data Centre, CCDC no. 149119 for complex **I**, CCDC no. 149076 for complex **II**, CCDC no. 149077 for complex **III**, CCDC no. 149078 for complex **IV** and CCDC no. 149080 for complex **V**. Copies of this information may be obtained free of charge from the Director, CCDC, 12 Union Road, Cambridge, CB2 1EZ, UK (fax: +44-1223-336033; e-mail: deposit@ccdc.cam.ac.uk or <http://www.ccdc.cam.ac.uk>).

Acknowledgements

Research funded in part by US Civilian and Development Foundation (grant REC-008), RFBR (grant 00-03-32987), and Integration Program.

References

- [1] A. Caneschi, D. Gatteschi, P. Rey, *Prog. Inorg. Chem.* 39 (1991) 331.
- [2] A. Caneschi, D. Gatteschi, J. Laugier, L. Pardi, P. Rey, C. Zanchini, *Inorg. Chem.* 27 (1988) 2027.
- [3] A. Caneschi, D. Gatteschi, J. Laugier, P. Rey, R. Sessoli, C. Zanchini, *J. Am. Chem. Soc.* 110 (1988) 2795.
- [4] A. Caneschi, D. Gatteschi, P. Rey, R. Sessoli, *Inorg. Chem.* 27 (1988) 1756.
- [5] A. Caneschi, F. Ferraro, D. Gatteschi, P. Rey, R. Sessoli, *Inorg. Chem.* 29 (1990) 4217.
- [6] A. Caneschi, D. Gatteschi, J. Laugier, P. Rey, R. Sessoli, *Inorg. Chim. Acta* 184 (1991) 67.
- [7] F. Lanfranc de Panthou, E. Belorizki, R. Calemczuk, D. Luneau, C.h. Marcenat, E. Ressouche, P.h. Turek, P. Rey, *J. Am. Chem. Soc.* 117 (1995) 11247.
- [8] S. Vasilevsky, E. Tretyakov, O. Usov, Yu. Molin, S. Fokin, Yu. Shwedenkov, V. Ikorskii, G. Romanenko, R. Sagdeev, V. Ovcharenko, *Mendeleev Commun.* (1998) 216.
- [9] E. Ulman, J. Osiecki, D.G.B. Boocock, R. Darcy, *J. Am. Chem. Soc.* 94 (1972) 7049.
- [10] V. Ovcharenko, S. Fokin, P. Rey, *Mol. Cryst. Liq. Cryst. (A)* 333 (1999) 109.
- [11] V.I. Ovcharenko, S.V. Fokin, G.V. Romanenko, I.V. Korobkov, P. Rey, *Izv. Akad. Nauk. Ser. Khim.* 108 (1999) 1539.
- [12] J.S. Smart, *Effective Fields Theories of Magnetism*, W.B.Saunders Company, Philadelphia, London, 1966.
- [13] A.B. Burdukov, V.I. Ovcharenko, V.N. Ikorskii, N.V. Per-vukhina, N.V. Podberezskaya, I.A. Grigor'ev, S.V. Larionov, L.B. Volodarsky, *Inorg. Chem.* 30 (1991) 972.
- [14] B. Bleaney, K.D. Bowers, *Proc. R. Soc. A* 214 (1952) 451.
- [15] Yu.V. Rakitin, V.T. Kalinnikov, *Modern Magnetochemistry*, Nauka, St. Petersburg, 1994, p. 272.